Am J Transl Res 2020;12(11):7354-7366
www.ajtr.org /ISSN:1943-8141/AJTR0103990

Original Article

Loss of cochlear ribbon synapses in the early stage of aging causes initial hearing impairment

Wei Xiong, Shukui Yu, Ke Liu, Shusheng Gong

Department of Otolaryngology-Head and Neck Surgery, Beijing Friendship Hospital, Capital Medical University, Beijing, China

Received October 25, 2019; Accepted October 11, 2020; Epub November 15, 2020; Published November 30, 2020

Abstract: Hearing loss can occur with aging. However, there remains debate about which cochlear component is the most susceptible to aging insult and the consequent pathological events responsible for age-related hearing loss. In this study, we used C57BL/6J mice to mimic the process of aging, and the auditory brainstem response (ABR) thresholds of aging mice were examined at different stages of aging (1, 2, 4, and 6 months [M]). The lifespan of 4 M was considered to be the early stage of aging. Immunostaining combined with laser confocal microscopy was employed to identify RIBEYE/CtBP2, a marker of cochlear ribbon synapses, and a quantitative analysis of the synaptic ribbon was carried out. The function of the ribbon synapse was estimated by amplitude alterations of ABR wave I. Furthermore, endocytosis of the inner hair cells was also detected using the fluorescence labeling dye FM1-43. We found that the loss of ribbon synapses in the early stage of aging occurred prior to hair cell or auditory nerve loss and was the initial pathological change. Additionally, the loss of ribbon synapses, including the quantity and function of synapses, was found to correspond to the elevations of the hearing threshold across frequencies. Moreover, a significant reduction in the endocytosis function of the inner hair cells was identified in the early stage of aging. Therefore, our study indicated that the reduction of cochlear ribbon synapses occurred at an early stage of aging and could be responsible for the consequent hearing loss.

Keywords: Aging-related hearing loss, cochlea, endocytosis, inner hair cells, ribbon synapse

Introduction

Age-related hearing loss (ARHL), or presbycusis, is a progressive and pathological process that results from age-related degeneration of the cochlea and central auditory system [1]. It affects almost half of individuals over the age of 75 years [2]. It is characterized by significant elevations in the hearing threshold with reductions in speech discrimination and difficulty in localization of sound sources, particularly in noisy environments [3]. Previous studies have shown that the loss of outer hair cells (OHCs), damage to the stereocilia, and degenerated alterations of the auditory nerves are possible mechanisms underlying ARHL [4-7]. However, recent studies have reported that these degenerative morphological changes in the cochlea occur after the onset of the hearing disorder [8-10]. For example, specific noise exposure can cause hearing loss coupled with intact cochlear hair cells, stereocilia, and spiral ganglion neurons (SGNs) [11, 12], which suggests that other cochlear components may be responsible for hearing loss. Both the ototoxic drugs such as gentamicin, and noise exposure have been proposed to cause a loss of ribbon synapses, which account for hearing impairment [10, 13]. Ribbon synapses of the inner hair cells (IHCs), submicrometer, electron-dense structure tethering synaptic vesicles, are formed on the cochlea with a powerful function specialized for encoding acoustic signals with high temporal precision over long periods [14, 15]. It has been reported that aging cochlea could form unexpected folded endings in the postsynaptic nerve terminals [16, 17], suggesting that aging could affect the morphologies or function of ribbon synapses. However, it remains unclear whether the quantity and function of the ribbon synapse are initially disrupted and thus contribute to the consequent hearing loss during aging.

In this study, we aimed to verify whether cochlear ribbon synapses are vulnerable to aging insult in C57BL/6J mice, a widespread model for ARHL. We explored the correlation between

the number and function of ribbon synapses and the reduction of hearing function in the early stage of aging. We found that the loss of cochlear ribbon synapses is an initial pathological event in the early stage of aging, which causes hearing loss and may consequently induce loss or damage to other cochlear components, such as IHCs, and SGNs.

Materials and methods

Animals

Healthy SPF C57BL/6J mice aged 1, 2, 4, and 6 months (M) with no middle and inner ear disease were provided by Beijing Vital River Laboratory. The mice with documented dates of birth were randomly divided into four groups to record their hearing levels using the auditory brainstem response (ABR) thresholds at 1, 2, 4, and 6 M, respectively. All animal experiments were approved by the Animal Ethics Committee of Capital Medical University and performed strictly in accordance with the standards of the Animal Ethics Committee.

Assessment of auditory function

Auditory brain response tests were used to determine the ABR thresholds. The thresholds were based on the visibility and reproducibility of waves II and III. The mice underwent double-blind testing of the ABR thresholds using equipment from Tucker-Davis Technologies (TDT, America). SigGen/BioSig software (TDT, America) was used to generate specific acoustic stimuli and to amplify, measure, and display the evoked brainstem responses of anesthetized mice (ketamine, 100 mg/kg and xylazine, 10 mg/kg, intraperitoneal injection). The animals were kept warm with a heating pad in a soundproof shielded room during the ABR recordings. Subdermal needle electrodes were inserted at the vertex, ventrolaterally to both ears of the anesthetized mice. Specific auditory stimuli (click), with a recurrence rate of 20 beats/s, average superposition time of 1,024 s, scanning time of 20 min, and filtering wave bandwidth of 100-3,000 Hz, were delivered binaurally through plastic tubes in the ear canals. Evoked brainstem responses were amplified and averaged, and their wave patterns were electronically displayed. The auditory thresholds were obtained for each stimulus by varying the sound pressure level at 5 dB steps up and down to identify the lowest level at which an ABR pattern could be recognized. The ABR thresholds were determined for each stimulus frequency by identifying the lowest intensity that produced a reproducible ABR pattern on the computer screen (at least two consistent peaks).

Analysis of the amplitude of ABR wave I

The amplitude of ABR wave I was also analyzed in this study, including the starting negative (n) deflection and the following positive (p) deflection. The amplitude of wave I was defined as Ip-In (latency: 1.2-1.9 ms). An algorithm for the automated determination of the ABR amplitudes was programmed using MATLAB (MathWorks, Massachusetts, USA). The amplitudes of ABR wave I were derived from the individual ear responses to a stimulus of 90 dB for each stimulus frequency. The mice were sacrificed for morphological investigations after the auditory testing.

Cochlear tissue processing

After the ABR testing, the mice were sacrificed by cervical dislocation and decapitation, and the cochleae were quickly separated from the temporal bone to the culture dish with a 4% paraformaldehyde solution. Under a dissecting microscope, a hole was made at the apex of the cochlea, and the round and oval windows were opened with a needle. The cochlea was perfused with a 4% paraformaldehyde solution instead of lymph fluid via the apex. Then, the specimen was decalcified in a 10% ethylenediaminetetraacetic acid (EDTA) solution for 1.5 h. The cochlea shell was removed from the apex to the base in phosphate buffered-saline (PBS). The basilar membrane was harvested without the vestibular and tectorial membranes.

Immunostaining

The samples were washed three times in PBS and pre-incubated for 1 h at room temperature in a blocking solution of 10% normal goat serum in 0.01 M PBS with 0.25% Triton X-100. Next, the samples were incubated with a combination of antibodies (1) mouse anti-CtBP2 (1:500, Abcam, ab204663), (2) rabbit anti-myosin VIIa (1:300, Proteus Biosciences, 25-6790), (3) chicken anti-NF200 (neurofilament-200) antibody (1:500, Chemicon, AB5539), and incu-

bated at 4°C overnight. After incubation, the samples were washed in PBS three times and incubated with the appropriate secondary antibodies coupled to Alexa Fluors in the green, red channels at room temperature for 1 h. After incubation, the samples were washed in PBS three times, and approximately 40 μL of DAPI (4,6-diamidino-2-phenylindole; Santa Cruz) was applied to stain the nuclei in the dark. The samples were imaged directly using fluorescent microscopy to test the specificity of the primary antibody. After immunostaining, the micro-dissected pieces of the basal membrane were mounted on coverslips under a dissecting microscope.

Hematoxylin and eosin (H&E) staining

The cochlear tissue specimens were fixed with 4% paraformaldehyde in PBS overnight at 4°C. The specimens were decalcified for 12 h in 10% EDTA. The preparations were then dehydrated with graded alcohol series, cleared with xylene, and embedded in paraffin. Paraffin-embedded specimens were cut into 10-um-thick sections and stained with H&E.

Laser confocal microscopy and counting of the synaptic ribbons

The 488-nm and 568-nm excitation wavelengths were conducted using a 63 × oil immersion confocal microscope (TCS SP8 II; Leica Microsystems, Wetzlar, Germany). The sequence scan was conducted on all of the IHCs in view, and the scanning interval was set to 0.5 μm. In each region, counting was performed in all IHCs and OHCs that were identified within 2-3 microscopic fields, which typically produced a total of 9-11 IHCs. The total number of CtBP2-stained puncta (green) was divided by the total number of IHC nuclei to obtain the average number of ribbons for each IHC.

The full length of the basal membrane was normalized to 100%. The samples were collected at 30% in the cochlear length examined from the apex corresponding to 4 kHz, 50% from the apex corresponding to 8 kHz, 70% corresponding to 16 kHz, and 80-90% from the apex corresponding to 32 kHz according to a published cochlear frequency map [18, 19].

Quantification of the OHCs, IHCs, and SGNs

The presence of an IHC or OHC was defined as an intact, spherical nucleus located at the basal end of the cell. In the DAPI-stained tissue, the intact spherical nuclei were counted to estimate the number of hair cells (HCs). Care was taken when the tissue was photographed so that the nuclei in focus were HC nuclei and not the nuclei of nearby supporting cells.

Western-blot analysis

A western blot analysis was used to determine the CtBP2 levels in the cochleae of mice with aging. The temporal bone was removed from the base of the skull and freshly dissected in ice-cold Hank's balanced salt solution (HBSS, Gibco, 1491037) to harvest the cochleae. To extract the total protein, the cochlear tissue samples were pulverized and homogenized in ice-cold RIPA lysis buffer (G2002, Servicebio). Tissue debris was removed by centrifugation at 12,000 × g at 4°C for 10 min, and the supernatants were retained as the total protein fractions. The internal reference was β-actin (GB12001, Servicebio). The concentrations of primary antibodies were anti-CtBP2 (1:1000; Abcam, ab204663) and anti-β-actin (1:3000).

FM1-43 loading and imaging

FM1-43 dye was used to detect the endocytosis function of HCs [20]. The organs of Corti's in mice aged 2 and 6 M were dissected and placed in a chamber filled with HBSS without calcium that contained (in mM): 5.36 KCl, 141.7 NaCl, 1 $MgCl_2$, 0.5 $MgSO_4$, 10 HEPES, 3.4 L-glutamine, and 6.9 D-glucose, with a pH of 7.4 at 37°C. FM1-43 (Invitrogen, USA) was dissolved in dimethyl sulfoxide to obtain a stock solution with a concentration of 1 mM. Time-lapse z-stack series along the HCs longitudinal axis were collected using Delta Vision. Microscopy was performed using a water immersion objective (63 × 0.9) (Delta Vision Microscopy Imaging Systems, UK). All solutions were carbogen-charged and pre-warmed at 37°C before the experiments. For labeling at room temperature, the HCs were pre-incubated for 2 min in a plastic plate containing HBSS and then incubated with 1.3 mM FM1-43 for 5 min at room temperature. The sites and quantity of dye entry into the IHCs were observed using fluorescence microscopy. All images were obtained with identical settings on a confocal Delta Vision Microscopy Imaging Systems (UK). FM dyes were excited with the 488 nm line of a laser, and their emission was detected in the range of 500-700 nm by a photomultiplier tube.

Statistical analysis

All data regarding the thresholds of the ABR test and the number of ribbon synapses are

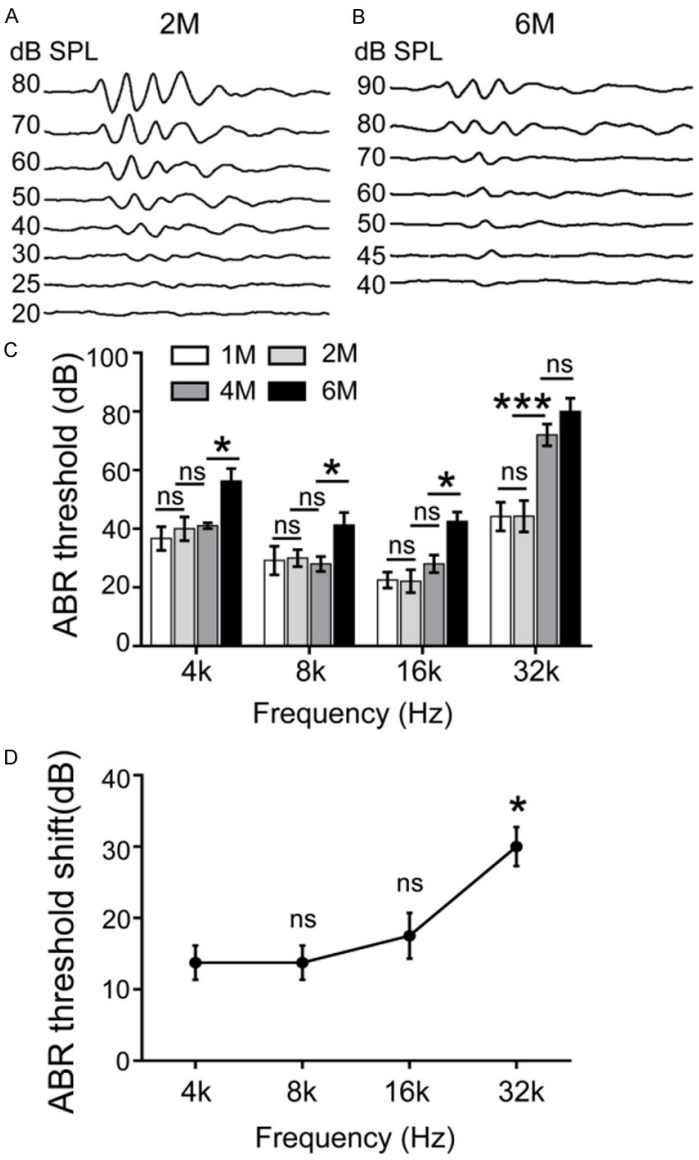

Figure 1. Changes in the ABR thresholds with aging. A. Representative image of the ABR waveform in 2 M mice (normal hearing threshold at 16 kHz), the lowest reproducible ABR waveform was 25 dB. B. Representative image of the ABR waveform at the same frequency in 6 M mice (there was significant elevation of the ABR threshold, which was 45 dB). C. The statistical analysis showed the significant elevation of the ABR threshold at 4, 8, and 16 kHz across frequencies between 4 M and 6 M mice (4 kHz: $P = 0.034$, t = 3.478, df = 3.331; 8 kHz: $P = 0.0443$, t = 2.664, df = 5.04; 16 Hz: $P = 0.0142$, t = 3.291, df = 6.682). No difference was seen in 32 kHz (32 kHz: $P = 0.2221$, t = 1.355, df = 6.265). There was no significant difference in the ABR threshold across frequencies between 1 and 2 M mice and 2 and 4 M mice except at the higher frequency of 32 kHz. ($P = 0.0005$, t = 6.518, df = 6.315) (*$P < 0.05$, **$P < 0.01$, ***$P < 0.001$). D. The ABR threshold shift between 2 and 6 M mice across frequencies showed a significant reduction at higher frequencies (32 kHz) (16 kHz vs. 32 kHz: $P = 0.0237$, t = 2.953, df = 6.391) compared to lower frequencies (4, 8, and 16 kHz; 4 kHz vs. 8 kHz: $P = 0.6737$, t = 0.4472, df = 4.927; 8 kHz vs. 16 kHz: $P = 0.2277$, t = 1.414, df = 4.154) (*$P < 0.05$), suggesting rapid hearing loss at the high-frequency with aging. (1 M: n = 6; 2 M: n = 6; 4 M: n = 5; 6 M: n = 5).

presented as the mean ± standard deviation (x ± SD). Plotting was performed using GraphPad Prism version 7. The statistical analysis for all experiments was performed using a two-tailed Student's *t*-test. A parametric test was used after normal distribution, and homogeneity of variance assumptions were satisfied. Homogeneity of variance was analyzed by F testing. If unequal variances in the comparisons were found, then we used the Welch-Satterthwaite formula to calibrate the degree of freedom and boundary value. The levels of significance were as follows: *$P < 0.05$, **$P < 0.01$, ***$P < 0.001$.

Results

Progressive and frequency-dependent elevations in the hearing threshold occurred at an early stage of aging

In this study, the ABR thresholds were examined at 4, 8, 16, and 32 kHz at different time points. The ABR analysis showed normal hearing in young mice across the frequencies (**Figure 1A-C**, age = 1 and 2 M). Our study showed that significant elevations in the hearing threshold initially appeared at a high-frequency (32 kHz) at 4 M and across frequencies at 6 M (**Figure 1B**, **1C**, age = 4 and 6 M, $P < 0.05$). To examine whether there are frequency-dependent differences of threshold shifts, tone burst testing was employed, and the mean threshold shifts at 4, 8, 16, and 32 kHz were obtained, respectively (4 kHz: 13.7±4.7 dB, 8 kHz: 12.5±2.8 dB, 16 kHz: 17.5±6.4 dB, 32 kHz: 27.5±2.8 dB). We found that there are more significant elevations of the ABR threshold shift at the cochlear region of higher frequencies (**Figure 1D**, 32 kHz, *$P < 0.05$) compared with the lower cochlear region (4, 8, and 16 kHz, respectively. $P < 0.05$) between mice aged 2 and 6 months.

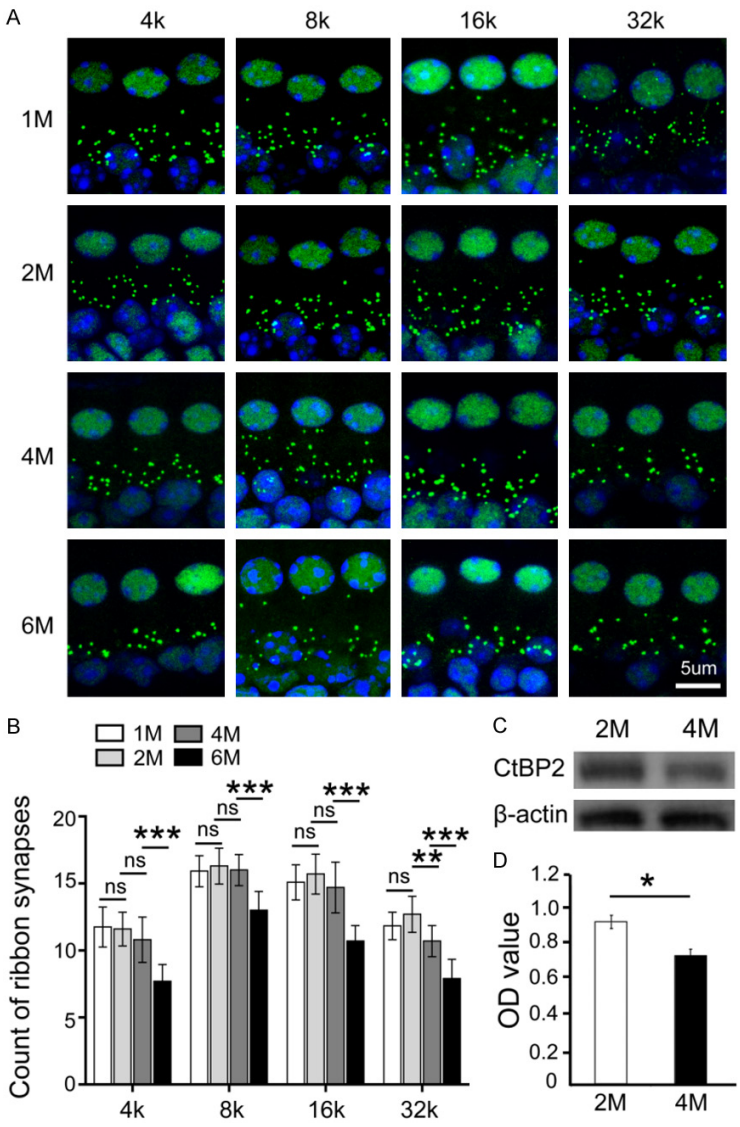

Figure 2. Dynamic changes of the cochlear ribbon synapses and immunohistochemistry of CtBP2 corresponding to the aging process. A. Representative image of the identification of cochlear ribbon synapses in mice (age: 1, 2, 4, and 6 M, respectively). The ribbon synapses are identified using anti-CtBP2 (green) and the nuclei of the IHCs stained by DAPI in blue. The nuclei of the IHCs were also stained by anti-CtBP2. Scale bar = 5 um. There was a significant reduction of CtBP2 immunofluorescence blotting at 32 kHz across the cochlear frequency map in 4 M mice, while the number of CtBP2 immunofluorescence blotting at 4, 8, and 16 kHz remained stable compared to the same cochlear region in 2 M mice. In 6 M mice, there was a significant reduction of CtBP2 immunofluorescence staining across frequencies in the cochlear map (4, 8, 16, and 32 kHz), n = 5. B. The statistical analysis showed that a significant loss of ribbon synapses initially occurred at a higher region of the cochlear frequency map in 4 M mice, and the loss of ribbon synapses across frequencies in 6 M mice. No significant difference in the CtBP2 immunofluorescence staining was seen between 1 and 2 M mice. C. CtBP2 expression in the cochlea of mice was measured using western blotting. A strong band of CtBP2 was identified in 2 M compared to 4 M mice. D. The quantitative analysis of CtBP2 expression showed a significant difference among 2 and 4 M mice. β-actin served as the loading control (n = 3).

Reduction of the cochlear ribbon synapses corresponding to the aging process

To explore whether the ribbon synapses changes correlated with the aging process, the number of ribbon synapses were examined using three-dimensional modeling combined with ribbon synapse labeling (identified as RIBEYE/CtBP2 immunostaining; **Figure 2A**). The quantification of synaptic puncta was performed at 1, 2, 4, and 6 M, respectively. We found that the number of ribbon synapses changed more significantly in the cochlear region of the higher frequency (32 kHz) compared to the lower-frequency region in the 4 M mice (**Figure 2B**, $P < 0.05$), suggesting that the earlier stage of aging could induce more significant loss of synapses in the high-frequency region compared with that in the cochlea.

In addition, this study carried out a similar statistical analysis of synapses on different turns of the cochlea of mice aged from 1 to 6 M. We found that younger mice (age: < 4 M) had an average number of synapses, and no significant change was observed throughout the length of the cochlea (**Figure 2B**, $P > 0.05$). For the mice aged 4 M, the number of synaptic markers was significantly reduced at the high-frequency cochlear regions, which corresponded to the basal turn (80% from apex, 32 kHz; **Figure 2B**, $P < 0.05$). For the mice aged 6 M, the number of synaptic markers decreased significantly across the frequencies. Our findings suggest that 4 M mice initially showed earlier and significant loss of hearing, coupled with an elevation of the ABR threshold at high-frequencies and a significant decrease in the number of ribbon synaps-

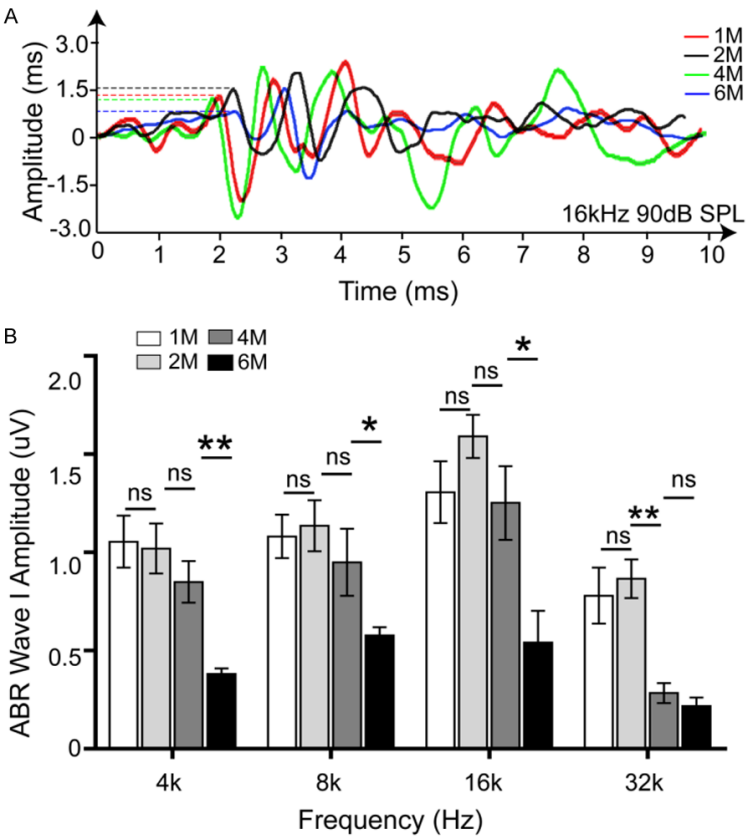

Figure 3. Reduction of the ABR I amplitude corresponded with the loss of ribbon synapses and elevated hearing threshold with aging. A. Representative waveform of the ABR wave I amplitude (16 kHz). There was a significant reduction of the ABR I amplitude in 6 M mice. B. The statistical analysis showed significant reductions of the ABR wave I amplitude at 32 kHz in 4 M mice compared to 2 M mice (32 kHz: $P = 0.0029$, t = 4.542, df = 6.781) and across frequencies in 6 M mice compared to 4 M mice, (4 kHz: $P = 0.0093$, t = 4.313, df = 4.579; 8 kHz: $P = 0.0219$, t = 3.143, df = 5.613; 16 kHz: $P = 0.0241$, t = 2.866, df = 7; 32 kHz: $P = 0.3494$, t = 1.003, df = 6.994) respectively, suggesting that the hearing loss and reduction of the ABR I amplitude, reflecting ribbon synapse functions, at 32 kHz in 4 M mice exhibited early ARHL (*$P < 0.05$, **$P < 0.01$, ***$P < 0.001$).

es. More significant alterations were found in the 6 M mice.

We performed further western blotting to determine the CtBP2 levels in the cochlea of mice with aging. A strong band of the pre-synapse marker, CtBP2, was found in the cochlear tissue of 2 M mice compared to 4 M mice, suggesting that the loss of synapses occurred during the early stage of aging (**Figure 2C**, **2D**, $P < 0.05$).

Reduction of the ABR I amplitude correlates with the loss of ribbon synapses with aging

To verify whether the loss of ribbon synapses correlates with the reduction of ABR I amplitude, we then examined the changes in ABR I amplitude across the frequencies (4, 8, 16, and 32 kHz) in mice aged 1, 2, 4, and 6 M, respectively. There were no significant reductions across the frequencies in the mice aged 1 and 2 M. Significant reductions in the ABR I amplitude were initially identified at 32 kHz in mice aged 4 M. Meanwhile, amplitude reductions occurred across frequencies in the mice aged 6 M compared to the mice aged 2 M (**Figure 3**, $P < 0.05$), suggesting that functional disruption may initially occur at 32 kHz in mice aged 4 M.

Loss of ribbon synapses occurred prior to the morphological alterations of the cochlear components

To investigate whether the loss of the ribbon synapses occurred prior to the morphological changes in the major component of the cochlea, we examined the HCs, SGNs, and their cochlear nerve terminals. We found that there was almost normal morphology in both cochlear HCs and SGNs and its innervated neurofilaments in 1, 2, and 4 M mice (**Figure 4A-C**). In mice aged 6 M, loss of OHCs and SGNs rather than IHCs were identified (**Figure 4D**, **4E**), suggesting that the loss of ribbon synapses occurred prior to alterations of cochlear HCs and SGNs and its neurofilament in 4 and 6 M mice. Therefore, cochlear ribbon synapses were found to be more sensitive to aging insult.

Endocytosis function in the cochlear inner HCs decreases with aging

Next, we investigated the endocytosis function of the IHCs in mice aged 2 and 6 M using FM1-43 dye, a fluorescence marker for endocytosis. We found that compared to the IHCs in the mice aged 2 M, the fluorescence intensity of the IHCs in mice aged 6 M was decreased significantly both at 500 ms and 1000 ms, espe-

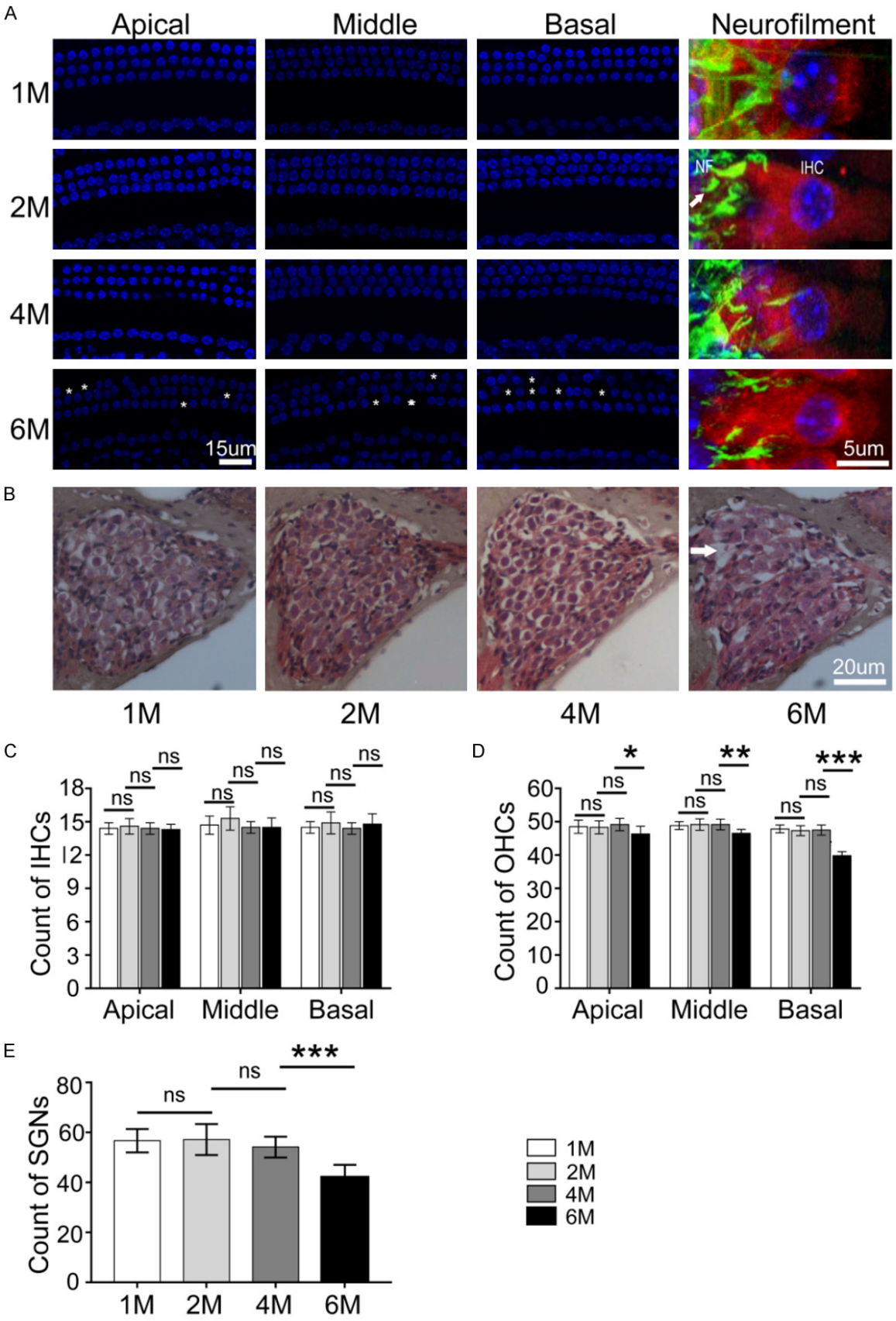
A
Apical
Middle
Basal
Neurofilment
1M
2M
4M
6M
NF
IHC
15um
5um
B
20um
1M
2M
4M
6M
C
Count of IHCs
ns
Apical
Middle
Basal
D
Count of OHCs
*
**
***
E
Count of SGNs
1M
2M
4M
6M

Figure 4. Gross morphologies of the cochlear components that remained intact during the early stage of aging. A. Left panel: Cochlear basal membrane at the apical, middle, and basal turn. Immunostaining and neurofilament immunostaining of IHCs and SGNs in 1, 2, 4, and 6 M mice. Images of neurofilament immunostaining were collected in the basal turn. Well-arranged HCs are represented by the three rows of OHCs and one row of IHCs in the 1, 2, and 4 M mice while the loss of OHCs occurred in mice aged 6 M across frequencies. (Asterisk) hair cell nucleus was stained by DAPI (blue). Scale bar = 15 um. Right panel: Enlarged image of the IHCs and adjacent terminals of SGNs (IHCs were stained using anti-myosin VIIa, in red; SGN neurofilaments were stained using anti-NF200, in green, white arrow, cell nucleus were stained by DAPI [blue]). There were no significant differences in neurofilament density at 1, 2, and 4 M, but a significant reduction of neurofilament density was observed in 6 M mice. Scale bar = 5 um. B. H&E staining of SGNs in the cochlear basal turn at 1, 2, 4, and 6 M. Loss of SGNs was identified in the cochlea at 6 M (white arrow), while no SGN loss was identified in 1, 2, and 4 M mice. Scale bar = 5 um. C. Quantification of the IHCs in 1, 2, 4, and 6 M mice across frequencies. There was no statistical difference among the number of IHCs in mice aged 1, 2, 4, and 6 M. D. Quantification of the OHCs in mice aged 1, 2, 4, and 6 M. No statistical difference was found among the number of OHCs in mice aged 1, 2, and 4 M, while the significant loss of OHCs was identified in 6 M mice compared to 4 M mice across frequencies (apical turn: $P = 0.043$, t = 2.335, df = 9.465; middle turn: $P = 0.0097$, t = 3.239, df = 9.356; basal turn: $P < 0.0001$, t = 9.807, df = 9.391) n = 5; E. Quantification of the SGNs in mice aged 1, 2, 4, and 6 M. No significant difference was found among the number of SGNs in mice aged 1, 2, and 4 M, while the loss of SGNs was identified in 6 M mice compared to 4 M mice ($P = 0.0014$, t = 4.95, df = 7.427), n = 5.

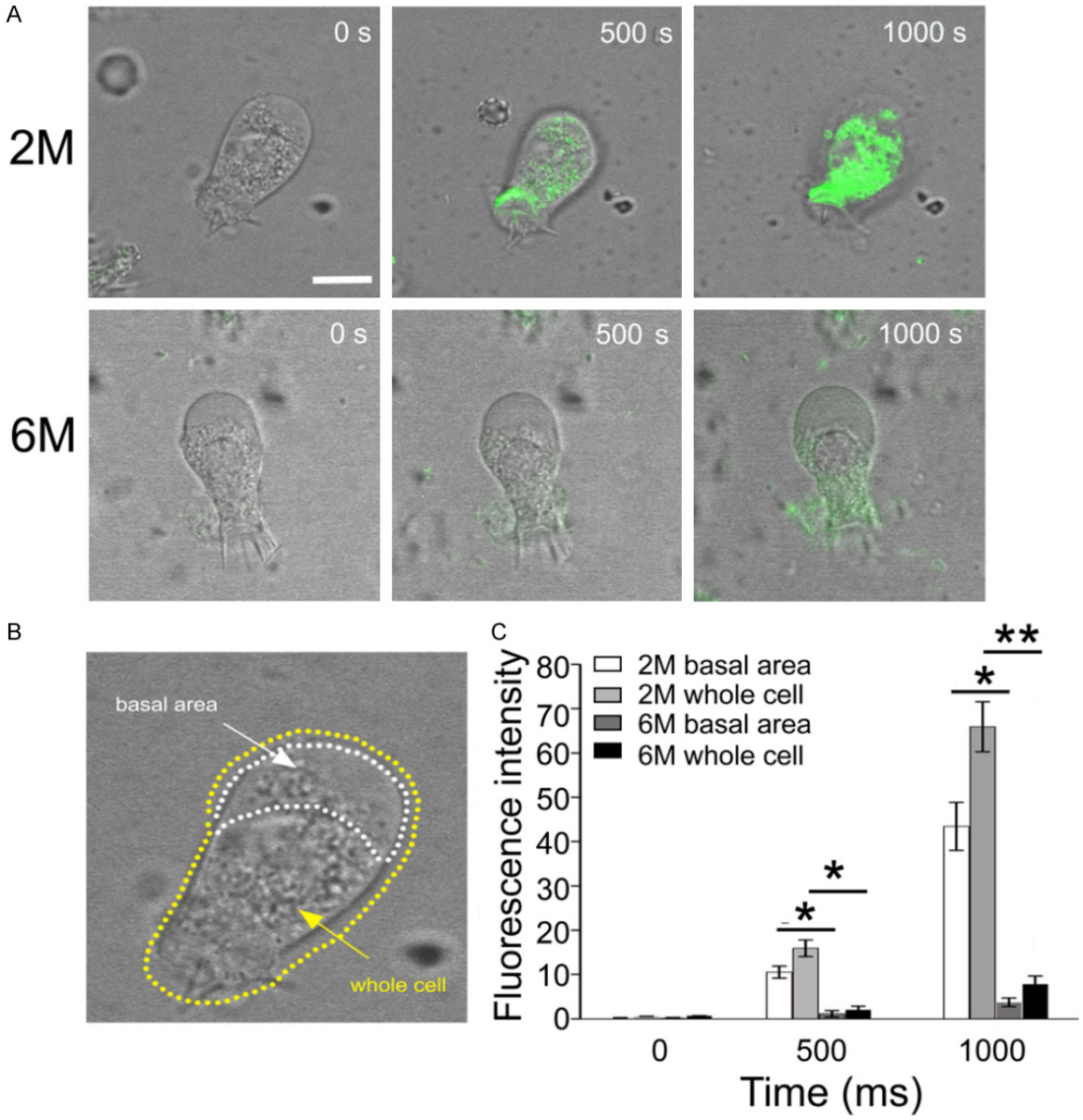

Figure 5. FM1-43 dye uptake in the IHCs in 2 and 6 M mice. A. The upper panel shows the velocity of FM1-43 dye entry into the IHCs in 2 M mice. The lower panel shows the FM1-43 dye uptake in the IHCs in 6 M mice. The 0 ms, 500 ms, and 1000 ms durations were imaged separately. The fluorescence intensity in the IHCs in 2 M mice was higher than that in 6 M mice. The fluorescence intensity is mostly concentrated in the basal area of the IHCs. Scale bar = 5 um. B. Sketch map to illustrate the active basal area of the IHCs (white dotted line) and the whole-cell area (yellow dotted line). C. Quantification of the fluorescence intensity of FM1-43 in the basal and whole-cell areas of the IHCs in 2 and 6 M mice, respectively. Compared to the IHCs in 2 M mice, the fluorescence intensity in the IHCs of 6 M mice showed a significant decrease in both the basal and whole-cell areas at the same time point 500 ms and 1000 ms (500 ms basal area: $P = 0.0196$, t = 4.648, df = 2.941; 500 ms whole-cell area: $P = 0.0196$, t = 4.648, df = 2.941, 1000 ms basal area: $P = 0.0102$, t = 8.514, df = 2.189; 1000 ms whole-cell area: $P = 0.0018$, t = 15.27, df = 2.424). $^{*}P < 0.05$, $^{**}P < 0.01$ (n = 3).

cially at the basal end of the IHCs. This is also called the 'pre-synaptic active zone'. Therefore, these results suggest a decline in the endocytosis function of IHCs with aging (**Figure 5**).

Discussion

ARHL is a progressive, irreversible, and symmetrical bilateral neurosensory hearing loss that results from the degeneration of either the peripheral auditory system or central auditory system [21]. Loss of cochlear HCs and SGNs, which are keys to the function of the cochlea, is thought to be the main reason for ARHL [22, 23]. Both HCs and SGNs are susceptible to injury, including direct mechanical and mitochondrial oxidative injury from noise and ototoxic drugs over time. However, an increasing number of novel findings have suggested that ribbon synapse loss may also be a key contributor [24, 25]. Ribbon synapses formed between IHCs and the peripheral end of SGNs are the first afferent neuronal connection in the auditory nervous system [26]. Incomplete recovery of ribbon synapses, together with no decline in the ABR threshold after noise damage, was found to be associated with a phenomenon known as hidden hearing loss [27, 28]. Our study showed that the loss of cochlear ribbon synapses corresponds to hearing impairment at the early stage of aging. Aging insult causes progressive and frequency-specific elevations of the hearing threshold. A more significant loss of the ribbon synapse was found at a higher frequency (32 kHz), corresponding to the cochlear region of the basal turn. Functional loss of ribbon synapses correlated with the reduced amplitude of ABR wave I and corresponded with the elevation of the ABR threshold. The loss of ribbon synapses occurred prior to morphological changes in cochlear components, including HCs and SGNs.

Sergeyenko et al. examined age-related cochlear synaptopathy in CBA mice [29]. While we found a similar result that ARHL was correlated with cochlear components such as OHCs, IHCs, and spiral ganglion cells, OHC losses preceded the loss of IHCs, and IHC loss was minimal in aging ears (80 weeks in CBA/J mice and 42 weeks in C57 mice in our study). Loss of spiral ganglion cells, the cell bodies of auditory nerve fibers, was slowly progressive throughout the life span and relatively uniform along the cochlear spiral. However, unlike Sergeyenko's results that OHC loss appeared first in apical, low-frequency cochlear regions but gradually reached the basal high-frequency regions, we found that losses of OHC and IHC ribbon synapses initially appeared in the basal turn of the cochlear regions, corresponding to the ABR threshold shift that initially appeared at high-frequencies in C57BL/6J mice.

Reduction of cochlear ribbon synapses is a primary pathological event at the early stage of aging

Loss of cochlear HCs has been observed in older mice and has been proposed to be a pathological reason contributing to ARHL [30]. However, it remains unclear as to whether synaptic connections between the IHCs and spiral ganglion cells are affected by aging, particularly at the early stage of aging (2-4 M in C57 mice). We examined the morphologies of the cochlear HCs as well as innervations between the IHCs and SGNs, and no significant changes were found in the mice aged 2, 4, and 6 M. Further, there were no significant differences in the quantity of IHCs and OHCs at 2, 4, and 6 M. Thus, no obvious morphological alterations were identified at the early stage of aging in this study. The evidence detailed above shows that significant morphological changes in the cochlea are not account for initial hearing loss in mice.

However, pathological changes should occur as an initial factor at the early stage of aging to

induce the consequent hearing loss. For example, in the central nervous system, a decrease in synaptic density and an increase in synaptic size have been documented with aging [31, 32]. Liberman et al. reported similar results in aging CBA mice. They found that the structure of afferent terminals and their synapses with IHCs differed between young-adult and older mice, indicating that synaptic reorganizations may partly account for the mechanism underlying ARHL [33]. Alternatively, synaptic changes are documented to be more susceptible to multiple traumatic stimuli, such as noise, drugs, and aging [34-36].

Thus, we assumed that the IHC ribbon synapses might be influenced in the initial stage of aging. The present study confirmed this hypothesis, with a significant reduction of IHC synapses at higher frequencies occurring even in mice aged 4 M. Taken together, our study provides robust evidence that aging exerts a negative effect on the ribbon synapses rather than the other cochlear components such as OHCs, IHCs, and SGNs. In this study, we did not count changes in the SGNs because we found a high density of SGN fibers and their endings in contact with the IHCs in the samples across age groups. SGN degeneration is usually associated with delayed damage during the aging process.

SGN degeneration could be a pathological basis of a distinct responsive reaction to the acoustic stimulations composed of varied frequency-sound proportions in the mice at the early stage of aging. In addition, a previous study reported a 50% reduction in afferent endings between younger (2 to 3 M) and older (10 to 12 M) C57 mice [37]. Francis et al. also proposed alterations of the SGN fiber terminals in C57 mice with aging. They found that abnormal folding structures appeared at the endings of fibers in the early stage of aging, suggesting a functional decline induced by aging [38], and thus revealed the possibility that synaptic changes could be induced by aging. However, in the above study, no immunostaining was used to identify the synapses, and it lacked functional estimations of the synaptic connections.

We carried out a functional estimation of the IHC ribbon synapses in aging mice. Compound auditory potential (CAP) or ABR wave I was reported to reflect the functional level of synaptic connections between the IHCs and endings of the spiral ganglion nerves *in vivo* [39, 40]. The function of the ribbon synapse can be roughly evaluated by CAP because CAP can reflect the summating potential between the inner HCs and auditory nerve endings in the cochlea. Further, the ABR waveform provides additional information to estimate the function of the IHC ribbon synapses *in vivo*. ABR wave I is generated between the IHCs and endings of the SGN fibers, reflecting excitability in the synaptic connection between the IHCs and SGNs [41, 42]. In contrast, the ABR I waveform may provide a further and more precise estimation of the functional ribbon synapse.

We found a significant reduction in the amplitude of ABR wave I initially at 32 kHz in the 4 M mice, suggesting that the functional decline of the cochlear ribbon synapses occurred prior to the changes in the synaptic areas by immunostaining. Thus, our data could be used to provide an early indicator of ARHL. These results are consistent with those of a previous report that the afferent synapses of IHCs are much more sensitive to ototoxicity exposure than other cochlear structures, such as OHCs, IHCs, and SGNs [43]. Moreover, a moderate level of noise exposure cannot cause loss of cochlear HCs, but it certainly can cause temporary hearing loss, coupled with irreversible recovery of IHC synapses [37]. Taken together, this evidence shows that recovery of the ribbon synapse may serve as a structural basis for hearing restoration.

Loss of ribbon synapses is frequency selective and may contribute to the reduction of hearing susceptibility

The most synaptic reduction was identified at approximately 32 kHz, 80% from the apex end in the cochlear length according to the cochlear frequency map [18]. We observed the differently aged mice (2 M and 6 M) and found that there is about a 38% loss of synapses at 32 kHz. In contrast, the loss of synapses is about 26%, 21%, and 33% at 16, 8, and 4 kHz, respectively. The functional analysis correspondingly showed that initial significant changes in the amplitude of ABR wave I were found at 32 kHz, suggesting that the functional decline of the cochlear ribbon synapses is also frequency selective. It could be that 32 kHz is the most sensitive frequency to sound stimuli.

Our additional study showed consistent data that there is a maximal number of IHC synapses formed around the cochlear tonotopic location corresponding to this specific frequency. However, it could not lead to the conclusion that this frequency is most susceptible to noise stimulation because we did not examine the proportions of spontaneous rate (SR) distribution in this study.

Hearing thresholds and susceptibility largely depend on the distributions of high or low SR fibers [44-46]. The greater prevalence of high-SR fibers at high-frequencies in mice could be responsible for the functional loss of hearing in background noise detected at early time points in aging mice [47]. Further, it may help explain the disruption of speech perception in older people in places with background noise.

Our study reveals that there could be a critical time window in which impaired hearing could be restored based on the damage and repair of cochlear ribbon synapses. A strategy could be to prevent ribbon synapses from attacks induced by ototoxic substrates, sound exposure, or genetic deficits. NT-3 has been proposed to have the potential to protect or restore damaged ribbon synapses. For example, Wang J et al. reported the successful delivery of NT-3 into cochlear inner HCs via a round window approach using AAV2 [48]. Therefore, potentially ARHL could be at least partially restored using a genetic therapy to achieve repair of the IHC ribbon synapses.

Conclusion

This study is the first to demonstrate that the loss of cochlear ribbon synapses at the basal turn of the cochlea, a subcellular structure, is the primary degenerating site and precedes the loss of IHCs and SGNs. Furthermore, this loss was found to correlate with the reduction in the amplitude of ABR wave I. Therefore, the loss of cochlear ribbon synapses might be a potential biochemical marker that could be used to identify the early stages of ARHL.

Acknowledgements

This work was supported by [the National Natural Science Foundation of China] under Grant [81830030]; [the National Natural Science Foundation of China] under Grant [81770997]; [the Beijing Science and Technology Commission - Education Commission Joint Fund Project] under Grant [KZ201810025040] and [the National Natural Science Foundation of China] under Grant [81771016].

Disclosure of conflict of interest

None.

Abbreviations

ABR, auditory brainstem response; ARHL, aging-related hearing loss; CAP, compound auditory potential; CtBP2, C-terminal binding protein 2; EDTA, ethylenediaminetetraacetic acid; IHC, inner hair cells; OC, organs of Corti's; OHC, outer hair cells; SPL, sound pressure level; SGNs, spiral ganglion neurons; PBS, phosphate-buffered saline; SR, spontaneous rate.

Address correspondence to: Ke Liu and Shusheng Gong, Department of Otolaryngology-Head and Neck Surgery, Beijing Friendship Hospital, Capital Medical University, 95 Yong'an Road, Beijing 100050, China. E-mail: liuke@ccmu.edu.cn (KL); gongss@ccmu.edu.cn (SSG)

References

[1] Makary CA, Shin J, Kujawa SG, Liberman MC and Merchant SN. Age-related primary cochlear neuronal degeneration in human temporal bones. J Assoc Res Otolaryngol 2011; 12: 711-717.

[2] Blackwell DL, Lucas JW and Clarke TC. Summary health statistics for U.S. adults: national health interview survey, 2012. Vital Health Stat 10 2014; 1-161.

[3] Gordon-Salant S. Hearing loss and aging: new research findings and clinical implications. J Rehabil Res Dev 2005; 42: 9-24.

[4] Liberman MC and Kiang NY. Acoustic trauma in cats. Cochlear pathology and auditory-nerve activity. Acta Otolaryngol Suppl 1978; 358: 1-63.

[5] Gates GA and Mills JH. Presbycusis. Lancet (London, England) 2005; 366: 1111-1120.

[6] Watson N, Ding B, Zhu X and Frisina RD. Chronic inflammation - inflammaging - in the ageing cochlea: a novel target for future presbycusis therapy. Ageing Res Rev 2017; 40: 142-148.

[7] Pickles JO, Osborne MP and Comis SD. Vulnerability of tip links between stereocilia to acoustic trauma in the guinea pig. Hear Res 1987; 25: 173-183.

[8] Kujawa SG and Liberman MC. Adding insult to injury: cochlear nerve degeneration after "tem-

porary" noise-induced hearing loss. J Neurosci 2009; 29: 14077-14085.
[9] Stamataki S, Francis HW, Lehar M, May BJ and Ryugo DK. Synaptic alterations at inner hair cells precede spiral ganglion cell loss in aging C57BL/6J mice. Hearing Res 2006; 221: 104-118.
[10] Liu K, Jiang X, Shi C, Shi L, Yang B, Shi L, Xu Y, Yang W and Yang S. Cochlear inner hair cell ribbon synapse is the primary target of ototoxic aminoglycoside stimuli. Mol Neurobiol 2013; 48: 647-654.
[11] Liberman MC. Noise-induced and age-related hearing loss: new perspectives and potential therapies. F1000Res 2017; 6: 927.
[12] Kobel M, Le Prell CG, Liu J, Hawks JW and Bao J. Noise-induced cochlear synaptopathy: past findings and future studies. Hearing Res 2017; 349: 148-154.
[13] Shi L, Liu L, He T, Guo X, Yu Z, Yin S and Wang J. Ribbon synapse plasticity in the cochleae of Guinea pigs after noise-induced silent damage. PLoS One 2013; 8: e81566.
[14] Fettiplace R. Hair cell transduction, tuning, and synaptic transmission in the mammalian cochlea. Compr Physiol 2017; 7: 1197-1227.
[15] Fuchs PA, Glowatzki E and Moser T. The afferent synapse of cochlear hair cells. Curr Opin Neurobiol 2003; 13: 452-458.
[16] Liberman MC and Kiang NY. Acoustic trauma in cats. Cochlear pathology and auditory-nerve activity. Acta Otolaryngol Suppl 1978; 358: 1-63.
[17] Liberman MC and Dodds LW. Single-neuron labeling and chronic cochlear pathology. III. Stereocilia damage and alterations of threshold tuning curves. Hearing Res 1984; 16: 55-74.
[18] Müller M, von Hünerbein K, Hoidis S and Smolders JW. A physiological place-frequency map of the cochlea in the CBA/J mouse. Hearing Res 2005; 202: 63-73.
[19] Yang L, Chen D, Qu T, Ding T, Yan A, Gong P, Liu Y, Zhang J, Gong S, Yang S, Peng H and Liu K. Maximal number of pre-synaptic ribbons are formed in cochlear region corresponding to middle frequency in mice. Acta Oto-Laryngol 2018; 138: 25-30.
[20] Li S, Yu S, Ding T, Yan A, Qi Y, Gong S, Tang S and Liu K. Different patterns of endocytosis in cochlear inner and outer hair cells of mice. Physiol Res 2019; 68: 659-665.
[21] Wang J and Puel JL. Presbycusis: an update on cochlear mechanisms and therapies. J Clin Med 2020; 9: 218.
[22] Ohlemiller KK and Gagnon PM. Apical-to-basal gradients in age-related cochlear degeneration and their relationship to "primary" loss of cochlear neurons. J Comp Neurol 2004; 479: 103-116.
[23] Bohne BA and Harding GW. Degeneration in the cochlea after noise damage: primary versus secondary events. Am J Otol 2000; 21: 505-509.
[24] Fernandez KA, Jeffers PW, Lall K, Liberman MC and Kujawa SG. Aging after noise exposure: acceleration of cochlear synaptopathy in "recovered" ears. J Neurosci 2015; 35: 7509-7520.
[25] Lin HW, Furman AC, Kujawa SG and Liberman MC. Primary neural degeneration in the Guinea pig cochlea after reversible noise-induced threshold shift. J Assoc Res Otolaryngol 2011; 12: 605-616.
[26] Meyer AC, Frank T, Khimich D, Hoch G, Riedel D, Chapochnikov NM, Yarin YM, Harke B, Hell SW, Egner A and Moser T. Tuning of synapse number, structure and function in the cochlea. Nat Neurosci 2009; 12: 444-453.
[27] Shi L, Chang Y, Li X, Aiken S, Liu L and Wang J. Cochlear synaptopathy and noise-induced hidden hearing loss. Neural Plast 2016; 2016: 6143164.
[28] Lin HW, Furman AC, Kujawa SG and Liberman MC. Primary neural degeneration in the Guinea pig cochlea after reversible noise-induced threshold shift. J Assoc Res Otolaryngol 2011; 12: 605-616.
[29] Sergeyenko Y, Lall K, Liberman MC and Kujawa SG. Age-related cochlear synaptopathy: an early-onset contributor to auditory functional decline. J Neurosci 2013; 33: 13686-13694.
[30] Bohne BA and Harding GW. Degeneration in the cochlea after noise damage: primary versus secondary events. Am J Otol 2000; 21: 505-509.
[31] Bertoni-Freddari C, Fattoretti P, Giorgetti B, Grossi Y, Balietti M, Casoli T, Di Stefano G and Perretta G. Alterations of synaptic turnover rate in aging may trigger senile plaque formation and neurodegeneration. Ann Ny Acad Sci 2007; 1096: 128-137.
[32] Todorova V and Blokland A. Mitochondria and synaptic plasticity in the mature and aging nervous system. Curr Neuropharmacol 2017; 15: 166-173.
[33] Liberman LD, Suzuki J and Liberman MC. Dynamics of cochlear synaptopathy after acoustic overexposure. J Assoc Res Otolaryngol 2015; 16: 205-19.
[34] Coyat C, Cazevieille C, Baudoux V, Larroze-Chicot P, Caumes B and Gonzalez-Gonzalez S. Morphological consequences of acoustic trauma on cochlear hair cells and the auditory nerve. Int J Neurosci 2019; 129: 580-587.
[35] Liberman MC and Kujawa SG. Cochlear synaptopathy in acquired sensorineural hearing loss: manifestations and mechanisms. Hearing Res 2017; 349: 138-147.
[36] Kujawa SG and Liberman MC. Adding insult to injury: cochlear nerve degeneration after "tem-

porary" noise-induced hearing loss. J Neurosci 2009; 29: 14077-14085.
[37] Kujawa SG and Liberman MC. Synaptopathy in the noise-exposed and aging cochlea: primary neural degeneration in acquired sensorineural hearing loss. Hearing Res 2015; 330: 191-199.
[38] Francis HW, Rivas A, Lehar M and Ryugo DK. Two types of afferent terminals innervate cochlear inner hair cells in C57BL/6J mice. Brain Res 2004; 1016: 182-194.
[39] Liberman MC and Kujawa SG. Cochlear synaptopathy in acquired sensorineural hearing loss: manifestations and mechanisms. Hearing Res 2017; 349: 138-147.
[40] Mehraei G, Hickox AE, Bharadwaj HM, Goldberg H, Verhulst S, Liberman MC and Shinn-Cunningham BG. Auditory brainstem response latency in noise as a marker of cochlear synaptopathy. J Neurosci 2016; 36: 3755-3764.
[41] Moser T and Starr A. Auditory neuropathy--neural and synaptic mechanisms. Nature reviews. Nat Rev Neurol 2016; 12: 135-149.
[42] Moser T, Predoehl F and Starr A. Review of hair cell synapse defects in sensorineural hearing impairment. Otol Neurotol 2013; 34: 995-1004.
[43] Schaette R and McAlpine D. Tinnitus with a normal audiogram: physiological evidence for hidden hearing loss and computational model. J Neurosci 2011; 31: 13452-13457.
[44] Schmiedt RA, Mills JH and Boettcher FA. Age-related loss of activity of auditory-nerve fibers. J Neurophysiol 1996; 76: 2799-2803.
[45] Rhode WS, Geisler CD and Kennedy DT. Auditory nerve fiber response to wide-band noise and tone combinations. J Neurophysiol 1978; 41: 692-704.
[46] Furman AC, Kujawa SG and Liberman MC. Noise-induced cochlear neuropathy is selective for fibers with low spontaneous rates. J Neurophysiol 2013; 110: 577-586.
[47] Prosen CA, Dore DJ and May BJ. The functional age of hearing loss in a mouse model of presbycusis. I. Behavioral assessments. Hearing Res 2003; 183: 44-56.
[48] Chen H, Xing Y, Xia L, Chen Z, Yin S and Wang J. AAV-mediated NT-3 overexpression protects cochleae against noise-induced synaptopathy. Gene Ther 2018; 25: 251-259.